SCIENTIFIC REPORTS

OPEN

SUBJECT AREAS:
ELECTRONIC PROPERTIES AND DEVICES
BIOMATERIALS - CELLS

Received
3 July 2014

Accepted
28 November 2014

Published
22 December 2014

Correspondence and requests for materials should be addressed to V.P. (vengadeshp@um.edu.my)

Reduced Graphene Oxide Anodes for Potential Application in Algae Biophotovoltaic Platforms

Fong-Lee Ng[1,2], Muhammad Musoddiq Jaafar[3], Siew-Moi Phang[1,2], Zhijian Chan[3], Nurul Anati Salleh[3], Siti Zulfikriyah Azmi[3], Kamran Yunus[4], Adrian C. Fisher[4] & Vengadesh Periasamy[3]

[1]Institute of Ocean and Earth Sciences (IOES), University of Malaya, 50603 Kuala Lumpur, [2]Institute of Biological Sciences, Faculty of Science, University of Malaya, 50603 Kuala Lumpur, Malaysia, [3]Low Dimensional Materials Research Centre (LDMRC), Department of Physics, University of Malaya, 50603 Kuala Lumpur, [4]Centre of Research for Electrochemical, Science and Technology (CREST), Department of Chemical Engineering and Biotechnology, University of Cambridge, New Museums Site, Pembroke Street, CB4 3RA Cambridge.

The search for renewable energy sources has become challenging in the current era, as conventional fuel sources are of finite origins. Recent research interest has focused on various biophotovoltaic (BPV) platforms utilizing algae, which are then used to harvest solar energy and generate electrical power. The majority of BPV platforms incorporate indium tin oxide (ITO) anodes for the purpose of charge transfer due to its inherent optical and electrical properties. However, other materials such as reduced graphene oxide (RGO) could provide higher efficiency due to their intrinsic electrical properties and biological compatibility. In this work, the performance of algae biofilms grown on RGO and ITO anodes were measured and discussed. Results indicate improved peak power of 0.1481 mWm^{-2} using the RGO electrode and an increase in efficiency of 119%, illustrating the potential of RGO as an anode material for applications in biofilm derived devices and systems.

Worldwide energy demand has increased rapidly due to expanding global population. The heavy reliance on fossil hydrocarbons has resulted in depletion of these natural resources. As a consequence, there is increased interest in the development of alternative energy sources such as hydroelectric, solar energy, wind energy, wave power, geothermal energy, artificial photosynthesis and tidal power[1]. In particular, solar powered technologies present an energy source[2] whereby the energy from sunlight are captured and exploited as a clean sustainable source of energy[3]. Photosynthesis presents an efficient and sustainable route for harvesting solar energy, and studies have reported the use of photosynthetic species that can be used to produce sustainable fuels and chemical feedstock[4].

One potential organism for alternative energy development is algae. These photosynthetic organisms successfully harvest the solar energy and convert it to chemical energy through photosynthesis[5,6] with fast growth rates, diverse products and tolerance to extreme environments[7]. The biomass productivity of microalgae was estimated to be 50 times higher than switch grass, which is the fastest growing terrestrial plant[8], and therefore microalgae are being investigated as feedstocks for biodiesel, bioethanol, biohydrogen and bioelectricity production[9]. Furthermore, recent studies have reported the use of microalgae in fuel cells (FCs), giving rise to a novel range of systems based on biological photovoltaic devices or biophotovoltaics (BPV)[10,11].

Pathways for electron transport during photosynthesis and how they can be intercepted is a key factor in improving the efficiency of BPVs[12]. Active compounds such as neutral red (NR) and methylene blue (MB) have been used as mediators between cells and electrodes[13]. Bombelli et al (2011)[10] have utilized various exogenous soluble mediator compounds to facilitate electron transfer, such as 5 mM ferricynide between the biological materials and the anode. Biological materials used in this study were *Synechocystis* cells and thylakoid membrane isolated from cells with total power output of 4.71 and 9.28 nWμmol Chl^{1} respectively. However, the active compounds inside the mediators are not appropriate for long-term operation of the BPV device[14]. In a more recent study, the use of exogenous mediators were replaced with the development of biofilms[15], and using a *Synechococcus* biofilm produced a peak power output of 10 mWm^{-2}. Biofilm development offers several advantages by reducing internal potential losses due to direct contact between cell and electrode, which contributes to the increase of power output. In addition, biofilms composed of microorganisms attached to surfaces such as

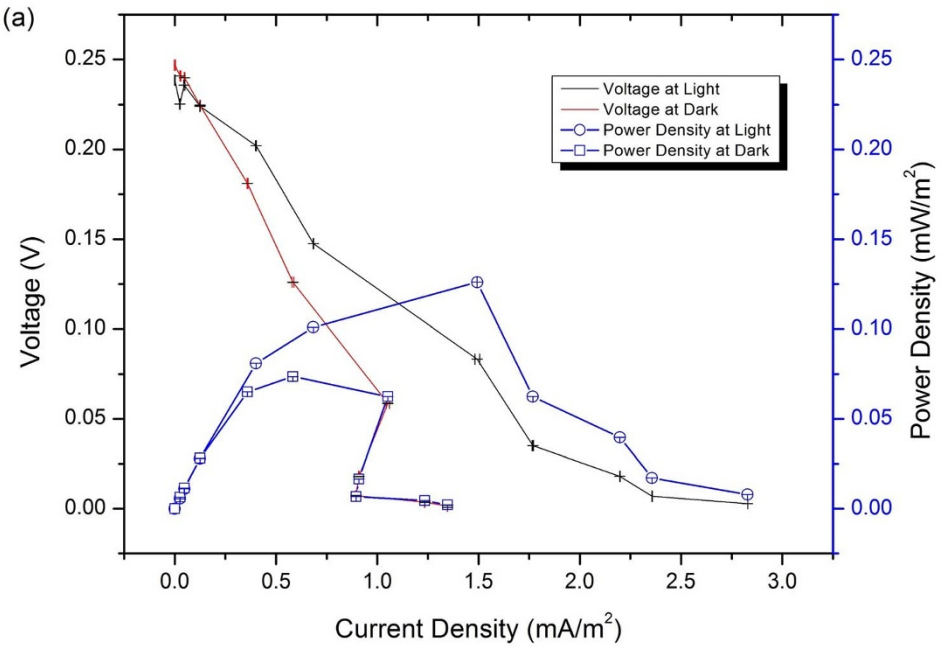

Figure 1 | **Polarization curves for the (a) ITO and (b) RGO based BPV devices.**

indium tin oxide (ITO) form a hydrated polymeric matrix consisting of polysaccharides, protein and nucleic acids[16], which could contribute to the overall interfacial properties of electron transport in biofilms.

ITO offers unique optical and electrical properties[17], due to it being an n-type semiconductor with low electrical resistivity and a wide band gap ($E_g > 4.1$ eV). It has been used widely in applications ranging from flat panel displays, solar cells and gas sensors[18]. Studies of biofilm growth and characterization in BPV devices have used ITO thin films as the anode material[19]. Even though the optical transparency offers many advantages for cultivating microalgae biofilms, the overall efficiency for electron transfer to the electrode surface remains a key limitation[20].

Over the past decades, carbon based electrodes have been reported for electrochemical sensing in a range of biological systems, from studies of enzyme metabolism to detection of proteins for biosensor applications[21]. In addition, graphene based electrode materials have demonstrated unique capabilities for electrical sensing of biological systems due to their inherent abundant functional groups[22,23]. Furthermore, graphene and graphene oxide (GO) layers have been in the mainstream research in recent years and actively investigated to replace and build new composite materials[24] mainly due to its high biocompatibility behavior. This behavior demonstrated by the presence of the oxygen-containing functional groups on the surface of reduced graphene oxide (RGO) or functionalized graphene sheets has been extensively reported containing functional groups[23,24,25] vital for the fabrication of electrochemical devices.

In this paper, a comparative study between ITO and RGO films developed using an in-house Langmuir-Blodgett (LB) technique was conducted. Biofilms of *Chlorella* sp. were cultivated on the electrodes surfaces and were used as the anode material within a BPV platform. The *Chlorella* sp. (UMACC 313) was selected from the University of Malaya Algae Culture Collection (UMACC) because of its inherent abilities to form biofilms[6] on substrates and was isolated from the aerobic pond for palm oil mill effluent (POME) treatment. Characterization of the BPVs were done using polarization curves, surface potential measurements and surface porosity imaging using Field Effect Scanning Electron Microscope (FESEM).

Results

Under illumination, the BPV power output shows increase for both anode electrodes (Fig. 1). However, a higher power output was observed on the RGO based BPV (1b). Peak power output for the RGO based BPV, measured at 0.273 mWm^{-2} (Table 1) was produced at a current density of 0.735 mAm^{-2}.

A direct comparison of the peak power outputs for both light and dark conditions between ITO and RGO based anodes can be seen (Fig. 2). In the dark cycle, there is an increase of 0.139 mWm^{-2} between ITO and RGO based electrodes. An increase of 0.1481 mWm^{-2} meanwhile was measured during the light cycle. This reflects to a relative power increase of 118.96% and 189.0% for the light and dark conditions respectively. The FESEM image (Fig. 3) shows the surface morphology of the RGO film being used to harvest the microalgae. It clearly shows the highly porous RGO surface with pores in the range of about 1.2 to 3.8 μm. Figure 4 meanwhile demonstrates the FESEM images of *Chlorella* sp biofilms on both ITO (a) and RGO (b) anodes. A higher number of algae cells lodged within the RGO pores can be clearly observed compared to when ITO anodes were used.

Table 1 | Maximum current density and maximum power density for ITO and RGO based BPV device in light and dark condition, data as means ± S.D. (n = 3)

Anode material	Condition	Maximum Current Density (mA/m^2)	Maximum Power Density (mW/m^2)
ITO	Light	2.3 ± 0.1	0.13 ± 0.03
	Dark	1.3 ± 0.4	0.07 ± 0.01
RGO	Light	2.0 ± 0.1	0.27 ± 0.03
	Dark	1.7 ± 0.4	0.21 ± 0.02

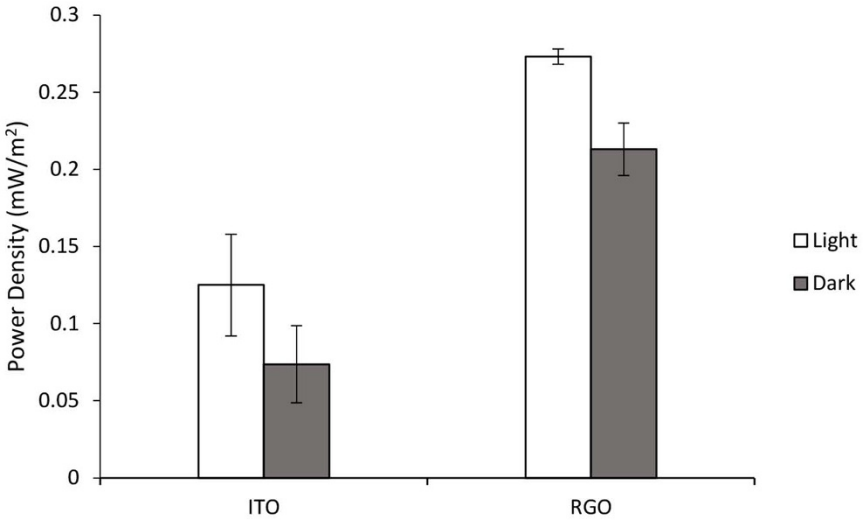

Figure 2 | **Direct comparison of peak power outputs for ITO and RGO based anode materials.**

The across the terminals in the RGO anode based BPV also demonstrated a higher value (510.70 ± 0.01 mV) compared to the ITO based anode (238.700 ± 0.002 mV) at open circuit potential when exposed to light. These were observed across the resistors as seen in Fig. 5. The RGO based electrode shows a significant increase of potential for all resistor values compared to ITO.

Discussion

Ng et al.[6] reported that there was significant power outputs revealed from biofilms of selected algae in BPV devices. Under irradiance, *Chlorella* sp. (UMACC 313) registered a power density of 0.124 mWm^{-2}, which was similar to the present results (0.125 mWm^{-2}). With a similar BPV device using biofilm of the Cyanophyte *Arthrospira maxima* on ITO, Inglesby et al.[26] reported very low power densities ranging from 6.7 to 24.8 μWm^{-2}. McCormick et al.[15] meanwhile replaced the use of exogenous mediators with the development of biofilms. Several algae were grown directly on an ITO-Polyethylene terephthalate (PET) anode on a sandwich type or an open-air design. This work demonstrated the ability to produce simple and portable BPV devices without the need of an artificial electron mediator. The *Synechococcus* biofilm in this work produced a peak power output at 1.03×10^{-2} Wm^{-2} under 10 Wm^{-2} of white light. Kumar et al[27] reported the power output from microbial fuel cells using different anode materials such as carbon, conductive polypyrrole (PPy), GO and RGO. The microorganisms in this study were *Escherichia coli* (ATCC 27325). The

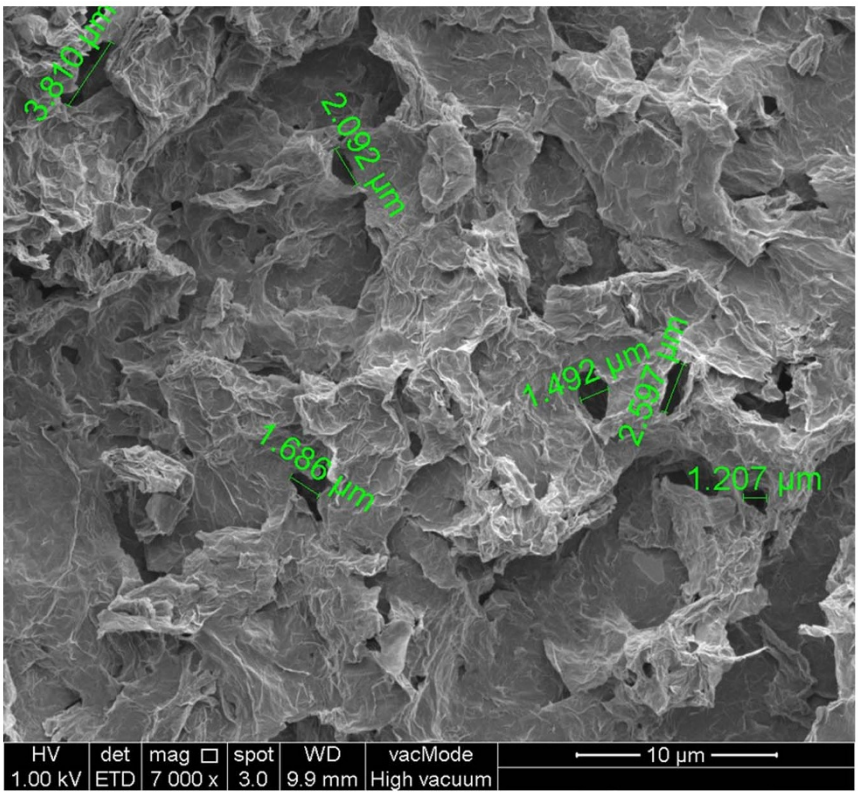

Figure 3 | **FESEM image of highly porous RGO surface in the range of about 1.2 to 3.8 µm.**

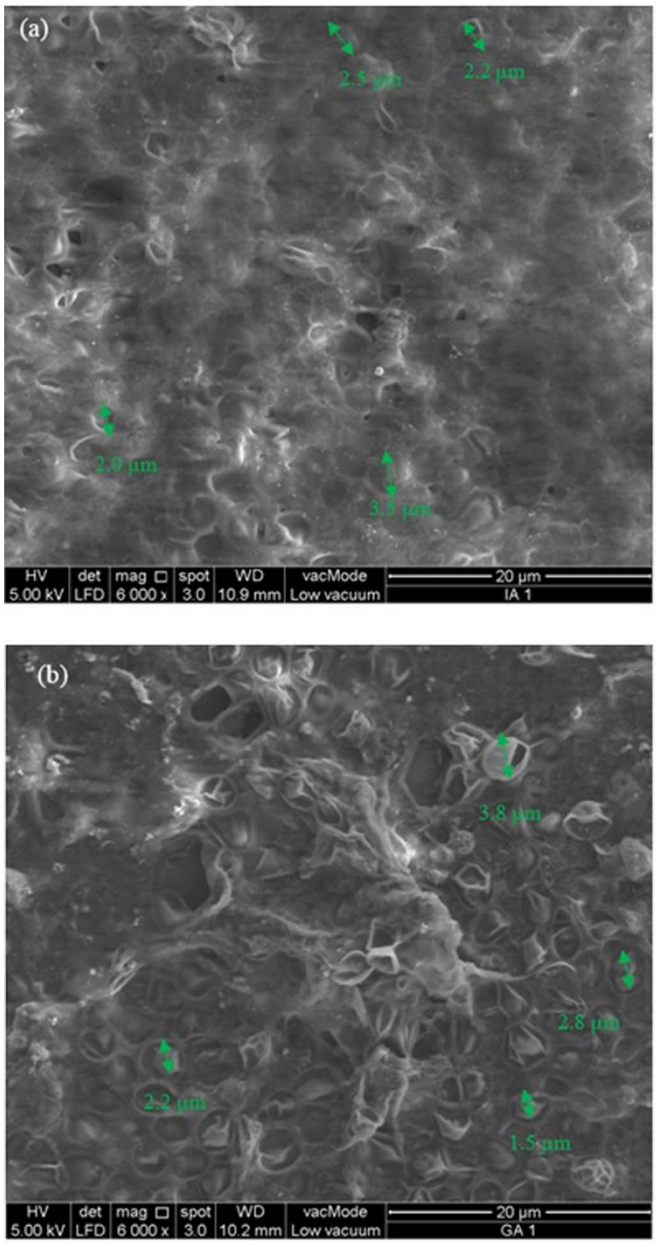

Figure 4 | FESEM images of *Chlorella* sp. (UMACC 313) biofilms grown on (a) ITO and (b) RGO anodes. The latter image shows high abundance of algae lodged within the correspondingly size micro pores.

authors demonstrated rapid increase of power densities in increasing order from bare carbon cloth, PPy, GO/PPy to rGO/PPy. (377 mW/m^2 < 615 mW/m^2 < 791 mW/m^2 < 1068 mW/m^2).

Increase in power output and potential for RGO based electrodes can be attributed to the unique properties of RGO. Highly porous film of RGO produced via LB method in this work allows for higher surface area and better attachment of biofilms. The presence of the functional groups on the RGO sheets also allows for easier and better attachments of the *Chlorella* sp. to the anode surface. This produces superior biocompatibility and hence a higher power output. Recent research shows that the three dimensional structure of surface topography such as pore size[28,29,30] and surface roughness[31] play an important role in cellular interaction and influence cell behavior. The dimensional size can be from micro to nanometers. As reported by Li et al., the porous structure of RGO could provide 3D microenvironments for cells to be able to resemble their in vivo counterparts[32]. These results in improved cellular communication, transportation of oxygen and nutrients and therefore removal of wastes and cellular metabolism on the structure are more efficient than those on 2D RGO films[25].

The pore sizes of the RGO film ranges from 1–4 µm (Fig. 3). The formation of pore sizes in this range is suitable for the growth and attachment of algae onto the films as also observed in Fig. 5. These may be attributed to ability of micro-scale cavities to securely harbor microalgae within the correspondingly sized porous cavities[33]. The presence of oxygen-containing functional groups on the surface of RGO sheets is also an important factor for biocompatibility properties[27,33]. These factors may contribute positively to the interaction between microalgae and the RGO film.

Furthermore when comparing the power curves for both light and dark cycles, a substantial contribution for power output was observed in the dark. This could be attributed to the metabolism of organic substrates stored within the algal cells or secreted out, during the dark phase[34,35]. Many species of *Chlorella* spp. carry out heterotrophic nutrition, which can lead to current production through oxidation of the organic compounds[35]. Since the *Chlorella* UMACC 313 was isolated from the organic palm oil mill effluent, it would certainly possess heterotrophic abilities[7]. *Chlorella* isolated from wastewater was found to be mixtrophic where organic compounds are also metabolised in the presence of light[36]. In addition when considering the power density for both ITO and RGO anodes, an increase of about 67% and 120% was observed when going from the dark to the light cycle. This may be the result of combined contributions of autotrophy (photosynthesis) and mixotrophy to current generation, in the light. Another factor may be the surface enhanced activity of the RGO anode material, which can be seen from the values of open circuit potential for RGO and ITO in both light and dark conditions (Figure 4)[27]. Although the power curves in Fig. 1a and b are predominately governed by mass transfer limitations, previous studies have shown that under different operating conditions the biofilm activity is spatially affected leading to enhanced electron flux at the electrode surface[26]. This could potentially lead to the deviation in the power curve observed at low resistor values and high current densities.

In conclusion, increase in the power density (118.96% and 189.0% for the light and dark cycles respectively) and open potential (114% and 107% for light and dark cycles respectively) was observed in RGO based BPV platform compared to conventional ITO based systems. These may be attributed to the functional-group enriched porous 3D structures of RGO, which provides suitable microenvironments for attachment, and growth of microalgae. The oxygen-containing functional groups in the RGO may also provide enhanced redox activities leading to more efficient electron transfer from the algae. However, a full understanding of the mechanism on the donation of electrons to the environment or charge transfer is yet to be fully understood. Nevertheless, the results obtained in this work demonstrate the potential of using RGO as electrode in BPV devices. Further work needs to be carried out to improve the power conversion efficiency of the device prior to development for possible commercial applications.

Methods

Fabrication of reduced graphene oxide anode using Langmuir-Blodgett method. High surface area RGO (Graphene Supermarket, USA) of 2.0 mg was mixed with 1.0 mL of polar solvent (99.9% pure methanol) in a 5.0 mL vile. The vial was sealed and sonicated up to 10 hours resulting in a suspension of RGO. Langmuir films of RGO were prepared using a round-type NIMA LB trough (model 2200) from NIMA Technology, UK that was carefully pre-cleaned using chloroform and methanol. The experiment was conducted in a clean and dusts free 1 K clean room environment (ISO class 6). The solution of RGO solvent was spread at a rate of 100 µL/minute on DI water surface up to 1000 µL by using a micro syringe (precision ±2 µL) to form a monolayer. A tissue wetted with methanol was carefully used to spread the methanol vapor from a distance of 0.5 cm from the monolayer to reduce clouded area of RGO on the water surface.

Surface pressure of RGO monolayer was observed by using a tensiometer attached to a filter paper (1.0 cm × 2.2 cm) during compression of the barriers (15.0 cm^2/

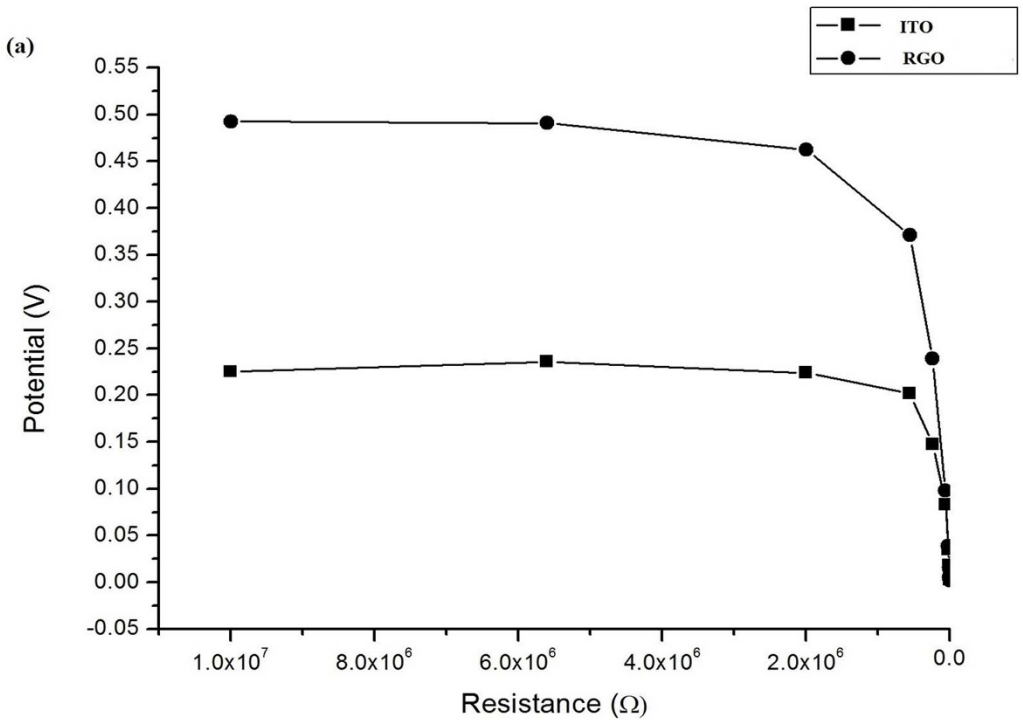

Figure 5 | **Comparison of potential across resistor for the (a) light cycles and (b) dark cycles.**

minute). Upon compression, the resulting isotherm graph was continuously monitored and recorded up to a target pressure of 10 mN/m. A glass substrate (3.5 cm × 3.5 cm) was then dipped vertically at a speed of 20 mm/minute. During the dip-coating process, the RGO monolayer was transferred onto the substrate. The prepared RGO film was then dried at 60°C in an oven for up to 12 hours to improve the adhesion of RGO layers preventing peeling-off of the underlying layers deposited. This process was repeated to obtain 6 sets of 6 coatings of the LB RGO films. The sheet resistance was calculated at 4.5×10^5 Ω/sq, while conductivity was measured at 2.74 S/m with a thickness of about 809 mm.

Algae biofilm formation. One strain was selected from the University of Malaya Algae Culture Collection (UMACC)[37] as potential candidate for use in the BPV

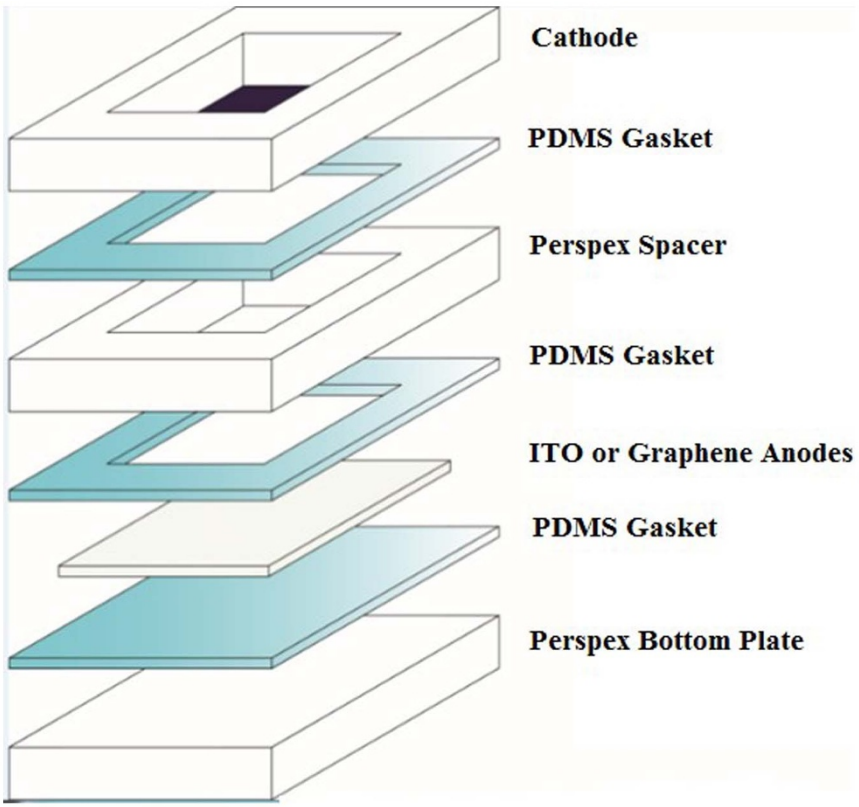

Figure 6 | **Exploded diagram of the BPV platform used in the study.**

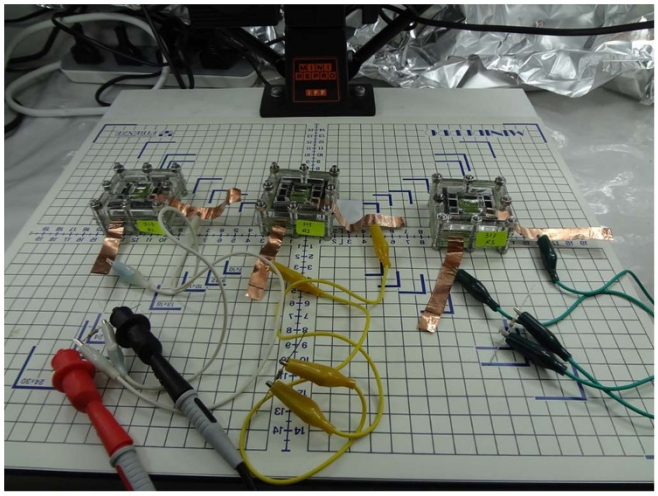

Figure 7 | BPV devices set up in triplicate. The biofilms on ITO and RGO were grown for 15 days until maximum surface area coverage was reached before setting-up the BPV device by inserting the algae biofilms and addition of fresh medium.

platforms. The green algae Chlorella sp. (UMACC 313) was grown in Bold's Basal Medium. 100 ml of exponential phase cultures of 0.5 (OD620 nm) were used. Cultures were placed into 200 ml sterile glass staining jars. ITO purchased from KINTEC, Hong Kong had a layer thickness of 100 nm with 377.0 Ω/sq and about 10^4 S/cm of sheet resistance and conductivity, respectively. ITO or RGO coated glass slides of dimensions (3.5 cm × 3.5 cm) were placed in the staining jar with the microalgae culture in triplicate. They were then transferred into an incubator at 24°C illuminated by cool white fluorescent lamps (30 μmol.$m^{-2}s^{-1}$) on a 12:12 hour light-dark cycle to allow for the algae biofilms to form on the slides. The algae biofilms took 15 days to reach optimum surface area coverage.

Biophotovoltaic device set up and electrical measurement. The RGO based BPV device used in this work was from an original ITO based platform developed by Centre for Research in Electrochemical Science and Technology (CREST), University of Cambridge. The closed, single-chamber BPV consisted of a (50 × 50) mm platinum-coated glass cathode placed in parallel with (3.5 cm × 3.5 cm) ITO or RGO coated glass (Fig. 6). Biofilms were grown on the surface (10 mm apart) in a clear Perspex chamber sealed with polydimethylsiloxane (PDMS) and the cavity filled with medium. The body of the open-air and single-chamber BPV was constructed of clear Perspex. Biofilms of *Chlorella* sp. grown on ITO and RGO coated glasses was then placed in the BPV device. Crocodile clips and copper wire served as connection between anode and cathode to the external circuit.

Prior to operation, the chambers were filled with fresh medium and maintained at 25°C. For light measurement, BPV devices were placed under irradiances of 30-μmol.photons.$m^{-2}s^{-1}$ for the duration of the experiments. For dark measurement, BPV devices were placed in a dark room and the device covered with a black cloth. To confirm the device was in the dark without any light source, a light meter (LI-250A, Licor) was used to detect the light intensity of the device environment and the reading was found to be zero. After dark adaptation for 15 minutes, current outputs were measured using a multimeter (Agilent U1251B). Polarization curves were generated for each strain by applying different resistance (10 MΩ, 5.6 MΩ, 2 MΩ, 560 KΩ, 240 KΩ, 62 KΩ, 22 KΩ, 9.1 KΩ, 3.3 KΩ and 1.1 KΩ) loads to the external circuit. To improve experimental accuracy and credibility, all measurements were carried-out in triplicates and their standard deviations recorded (Fig. 7).

1. Panwar, N. L., Kaushik, S. C. & Kothari, S. Role of renewable energy sources in environmental protection: A review. *Sust. Ener. Rev.* **15**, 1513–1524 (2011).
2. Miles, R. W., Hynes, K. M. & Forbes, I. Photovoltaic solar cells: An overview of state-of-the- art cell development and environmental issues. *Prog. Crys. Grow. Charac. Mat.* **51**, 1–42 (2005).
3. Waldau, A. J. *PV Status Report 2012* [14] (Office for Official Publication of the European Communities, Luxembourg, 2012).
4. Flexer, V. & Mano, N. From Dynamic Measurements of Photosynthesis in a Living Plant to Sunlight Transformation into Electricity. *Anal. Chem.* **82**, 1444–1449 (2010).
5. Xie, X. H., Li, E. L. & Kang, T. Z. Mediator toxicity and dual effect of glucose on the lifespan for current generation by Cyanobacterium Synechocystis PCC 6714 based photoelectrochemical cells. *J. Chem. Tech. Biotech.* **86**, 109–114 (2011).
6. Ng, F. L., Phang, S. M., Periasamy, V., Yunus, K. & Fisher, A. C. Evaluation of algal biofilms on Indium Tin Oxide (ITO) for use in biophotovoltaic platforms based on photosynthetic performance. *PLoS ONE* **9**, e97643 (2014); DOI:10.1371/journal.pone.0097643.
7. Phang, S. M. & Ong, K. C. Algal biomass production in digested palm oil mill effluent. *Biological Wastes*, **25**, 171–193 (1988).
8. Li, Y., Horsman, M., Wu, N., Lan, C. Q. & Calero, N. D. Biofuels from microalgae. *Biotech. Prog.* **24**, 815–820 (2008).
9. Vejeysri, V., Phang, S. M., Chu, W. L., Majid, N. A. & Lim, P. E. Lipid productivity and fatty acid composition-guided selection of *Chlorella* strains isolated from Malaysia for biodiesel production. *J Appl. Phycol.* **26**, 1399–1413 (2013).
10. Bombelli, P. *et al*. Harnessing solar energy by bio-photovoltaic (BPV) devices. *Comm. Agr. Appl. Biol. Sci.* **76**, 89–91 (2011).
11. Mao, L. & Verwoerd, W. Selection of organisms for systems biology study of microbial electricity generation: a review. *Int. J. Ener. Environ. Eng.* **4**, 1–18 (2013).
12. Jang, J. K. *et al*. Construction and operation of a novel mediator- and membrane-less microbial fuel cell. *Proc. Biochem.* **39**, 1007–1012 (2004).
13. Clauwaert, P. *et al*. Biological Denitrification in Microbial Fuel Cells. *Environ. Sci. Tech.* **41**, 3354–3360 (2007).
14. Fu, C. C., Hung, T. C., Wu, W. T., Wen, T. C. & Su, C. H. Current and voltage responses in instant photosynthetic microbial cells with *Spirulina platensis*. *Biochem. Eng. J.* **52**, 175–180 (2010).
15. McCormick, A. J. *et al*. Photosynthetic biofilms in pure culture harness solar energy in a mediatorless bio-photovoltaic cell (BPV) system. *Ener. Envir. Sci.* **4**, 4699–4709 (2011).
16. Sauer, K., Rickard, A. H. & Davies, D. G. Biofilms and Biocomplexity. *Microbe.* **2**, 347–353 (2007).
17. Martinu, L., Zabeida, O. & Klemberg-Sapieha, J. E. [Plasma-Enchance Chemical Vapor Depositions of Functional Coatings]. *Handbook of Deposition Technologies for Films and Coatings: Science, Applications and Technology* [Martin, P. M. (ed.)] [445] (Elsevier Inc., Philadelphia 2009).
18. Pokaipisit, A., Horprathum, M. & Limsuwan, P. Vacuum and air annealing effects on properties of Indium Tin Oxide films prepared by ion-assisted electron beam evaporation. Jap. *J. Appl. Phys.* **42**, 4692–4695 (2008).
19. Wen, A. J. C. *et al*. Effect of substrate angle on properties of ITO films deposited by cathodic arc ion plating with In–Sn alloy target. *Surf. Coat. Tech.* **198**, 362–366 (2005).
20. Dhere, R. G. *et al*. Electro-optical properties of thin indium tin oxide films: Limitations on performance. *Sol. Cells.* **21**, 281–290 (1987).
21. Yuyan, S. *et al*. Graphene based electrochemical sensors and biosensors: A review. *Electroanalysis.* **22**, 1027–1036 (2010).
22. Geim, A. K. & Novoselov, K. S. The rise of graphene. *Nat Mater.* **6**, 183–191 (2007).
23. Singh, G. *et al*. Near room temperature reduction of graphene oxide Langmuir–Blodgett monolayers by hydrogen plasma. *Phys. Chem. Chem. Phys.* **16**, 11708–11718 (2014).
24. Li, X., Wang, X., Zhang, L., Lee, S. & Dai, H. Chemically derived, ultra smooth graphene nanoribbon semiconductors. *Sci.* **319**, 1229–1232 (2008).
25. Fan, H. *et al*. Fabrication, mechanical properties, and biocompatibility of graphene-reinforced Chitosan composites. *Biomacromol.* **11**, 2345–2351 (2010).
26. Inglesby, A. E., Yunus, K. & Fisher, A. C. In situ fluorescence and electrochemical monitoring of a photosynthetic microbial fuel cell. *Phys. Chem Chem. Phys.* **15**, 6903–6911 (2013).
27. Kumar, G. G. *et al*. Synthesis, structural, and morphological characterizations of reduced graphene oxide-supported polypyrrole anode catalysts for improved microbial fuel cell performances. *ACS Sustainable Chem. Eng.* **2**, 2283–2290 (2014).
28. Singhvi, R., Stephanopoulos, G. & Wang, D. I. Effects of substratum morphology on cell physiology. *Biotech. Bioeng.* **43**, 764–771 (1994).
29. Brauker, J. H. *et al*. Neovascularization of synthetic membranes directed by membrane microarchitecture. *J. Biomed. Mat. Res.* **29**, 1517–1524 (1995).
30. Bobyn, J. D., Wilson, G. J., MacGregor, D. C., Pilliar, R. M. & Weatherly, G. C. Effect of pore size on the peel strength of attachment of fibrous tissue to porous-surfaced implants. *J. Bio. Mat. Res.* **16**, 571–584 (1982).
31. Clark, P., Connolly, P., Curtis, A. S., Dow, J. A. & Wilkinson, C. D. Topographical control of cell behaviour. I. Simple step cues. *Development* **99**, 439–448 (1987).
32. Li, N. *et al*. Three-dimensional graphene foam as a biocompatible and conductive scaffold for neural stem cells. *Sci. Rep.* **3**, 1604 (2013).
33. Wahid, M. H. Eroglu, E., Chen, X., Smith, S. M. & Raston, C. L. Entrapment of *Chlorella vulgaris* cells within graphene oxide layers. *RSC Adv.* **3**, 8180–8183 (2013).
34. Fu, C. C. *et al*. Effects of biomass weight and light intensity on the performance of photosynthetic microbial fuel cells with *Spirulina platensis*. *Biores. Tech.* **100**, 4183–4186 (2009).
35. He, Z., Kan, F., Mansfeld, L., Angenent, L. & Nealson K. Self-sustained phototrophic microbial fuel cells based on the synergistic cooperation between photosynthetic microorganisms and heterotrophic bacteria. *Environ. Sci. Technol.* **43**, 1648–1654 (2009).
36. Phang, S. M., Chui, Y. Y., Kumaran, G., Jeyaratnam, S. & Hashim, M. A. [High rate algal ponds for treatment of wastewater: a case study for the rubber industry]. *Photosynthetic Microorganisms in Environmental Biotechnology* [Kojima, H. & Lee, Y. K. (eds.)] [51–76] (Springer-Verlag, Hong Kong, 2001).

37. Phang, S. M. & Chu, W. L. *Catalogue of Strains, University of Malaya Algae Culture Collection (UMACC)* [36–37] (University of Malaya, Kuala Lumpur, 1999).

Acknowledgments

This work was supported by the High Impact Research Grant, (HIR; J-21002-73823), Fundamental Research Grants, FRGS (FP004/2013A and KPT1059-2012), University of Malaya Postgraduate Research Fund (PPP; PG051-2012B) and Knowledge Management Grant (RP001O-13SUS). We would also like to record our gratitude to the Ministry of Education, Malaysia for financial assistance (NQPF GAAA grant) made available through the HLCB Post-doctoral program (V.P.) and CREATE Singapore (A.F.,K.Y.).

Author contributions

V.P., K.Y., F.N. and S.P. conceived and designed the experiments. F.N., M.J., Z.C., N.S. and S.A. performed the experiments. V.P., F.N., K.Y., S.P., A.F., M.J. and Z.C. analyzed the data. V.P. and S.P. contributed reagents, materials and analysis tools. F.N., V.P., S.P., M.J. and Z.C. wrote the main manuscript text and prepared figures 1–7. All authors reviewed the manuscript.

Additional information

Competing financial interests: The authors declare no competing financial interests.

How to cite this article: Ng, F.-L. *et al.* Reduced Graphene Oxide Anodes for Potential Application in Algae Biophotovoltaic Platforms. *Sci. Rep.* **4**, 7562; DOI:10.1038/srep07562 (2014).